Mapping Radial Ocean Surface Currents in the Outer Core of Hurricane Maria From Synthetic Aperture Radar Doppler Measurements

Shengren Fan, Biao Zhang, *Senior Member, IEEE*, Vladimir Kudryavtsev, and William Perrie

***Abstract*—Spaceborne synthetic aperture radar (SAR) Doppler shift measurements have been used for remote sensing of ocean surface currents during nonstorm events. However, mapping strong currents under storm conditions is still a challenging and unsolved issue. In this study, we attempt to retrieve radial current velocities from Sentinel-1A SAR Doppler shifts acquired over the outer core regions of Hurricane Maria for the first time. In these areas, the maximum wind speed is 28.7 m/s. Doppler shifts arising from the scalloping effect are first calculated using a linear fitting method. The nonzero Doppler shift measurements over the land within SAR scenes are then used to estimate Doppler shifts caused by antenna electronic mispointing and residual error. Finally, we compute sea-state-induced Doppler shifts (wave Doppler) based on our recently dual copolarization Doppler velocity (DPDop) model. The retrieved radial current velocities are compared with collocated high-frequency radar measurements, and show a bias of 0.02 m/s and a root-mean-square error of 0.19 m/s. These results suggest that it is possible to retrieve reliable radial current velocities under high wind conditions, as the contributions of nongeophysical terms and sea state to the Doppler shifts can be accurately estimated and removed.**

***Index Terms*—Doppler shift, hurricane, ocean surface current (OSC), synthetic aperture radar (SAR).**

Manuscript received 19 September 2023; revised 24 November 2023 and 10 December 2023; accepted 15 December 2023. Date of publication 19 December 2023; date of current version 29 December 2023. This work was supported in part by the Joint Project between National Natural Science Foundation of China and Russian Science Foundation under Grant 42061134016, in part by the National Natural Science Foundation under Grant 42076181 and Grant 42076197, in part by the ESA MAXSS project–Marine Atmospheric eXtreme Satellite Synergy, in part by the Canadian Ocean Frontier Institute Module A, and in part by the SWOT—Surface Water and Ocean Topography. *(Corresponding author: Biao Zhang.)*

Shengren Fan is with the School of Marine Sciences, Nanjing University of Information Science and Technology, Nanjing 210044, China, and also with Satellite Oceanography Laboratory, Russian State Hydrometeorological University, 195196 St. Petersburg, Russia (e-mail: shengrenfan@gmail.com).

Biao Zhang is with the School of Marine Sciences, Nanjing University of Information Science and Technology, Nanjing 210044, China, also with the Southern Marine Science and Engineering Guangdong Laboratory (Zhuhai), Zhuhai 51900, China, and also with the Fisheries and Oceans Canada, Bedford Institute of Oceanography, Dartmouth B2Y 4A2, Canada (e-mail: zhangbiao@nuist.edu.cn).

Vladimir Kudryavtsev is with the Satellite Oceanography Laboratory, Russian State Hydrometeorological University, 195196 St. Petersburg, Russia (e-mail: kudr@rshu.ru).

William Perrie is with Fisheries and Oceans Canada, Bedford Institute of Oceanography, Dartmouth B2Y 4A2, Canada (e-mail: william.perrie@dfo-mpo.gc.ca).

Digital Object Identifier 10.1109/JSTARS.2023.3344591

I. Introduction

HURRICANES transfer large amounts of kinetic energy from the atmosphere to the upper ocean, which induces strong vertical mixing in the ocean mixed layer. Thus, they generate strong surface and subsurface currents, and impact the atmosphere and marine boundary layer through air–sea interactions, with feedbacks of moisture, momentum, mass, and including climate-related greenhouse gases, such as CO_2. Various instruments have been used to measure ocean currents during hurricanes, including airborne expendable current profilers [1], electromagnetic autonomous profiling explorer floats [2], underwater gliders and wave gliders [3], [4], uncrewed surface vehicles (e.g., saildrone) [5], [6], and surface drifters [7], [8]. These devices provide high-quality measurements of near-surface currents, depth-average currents, and current profiles, even under extreme weather conditions. However, they only provide measurements along the storm tracks. To better understand the upper ocean response and feedback to hurricanes, it is extremely desirable to acquire surface currents over large areas, under high winds (>20 m/s).

Spaceborne synthetic aperture radar (SAR) is a unique microwave sensor for monitoring the dynamic ocean environment due to its high-resolution, wide coverage, day and night, and all-weather observational capabilities. SAR cannot only measure radar returns from the ocean surface but also Doppler shifts associated with surface scattering facets. Envisat ASAR and Sentinel-1 Doppler shift measurements have been widely used to retrieve the radial ocean surface current (OSC) velocity [9], [10], [11], [12] during nonstorm events. The retrieval results have been compared with the collocated coastal high-frequency (HF) radar and surface drifter observations [13]. The comparison showed a bias of −0.08 m/s and a root-mean-square error (RMSE) of 0.25 m/s for HF radar, and −0.02 m/s and 0.24 m/s for drifter measurements, respectively. Under hurricane conditions, extreme wave heights would occur in the right-front quadrant of the storm because the waves are trapped in an "extended fetch" when the group velocity of the waves is approximately equal to the translation speed of the storm [14], [15]. Cross swell dominates in the majority of hurricane regions [16], [17]. Moreover, the strongest current is observed to the right side of the storm track [8], [18]. Thus, surface current retrieval under hurricane conditions is a challenging task. A previous study calculated the Doppler velocity under hurricane conditions using

RADARSAT-1 SAR raw data and directly compared the results with drifting buoy current measurements [19]. However, the study did not estimate or remove the contributions of wave motion to the Doppler velocity before conducting the validation.

SAR-measured Doppler shifts consist of both geophysical and nongeophysical components. The geophysical term relates to ocean surface motion induced by the sea state and underlying surface currents. The nongeophysical term is associated with antenna electronic mispointing, satellite attitude variation, the scalloping effect, and residual error. Therefore, the accuracy of the SAR radial OSC velocity retrievals relies on the precise estimation of Doppler shifts arising from sea state and nongeophysical terms. To obtain reliable measurements of radial current velocity, several empirical geophysical models (e.g., CDOP3S, CDOP3SX, and CDOP3SiX) have been proposed to estimate the contribution of sea state to the SAR Doppler shift [12], [20]. Recently, we have developed a dual copolarization Doppler velocity (DPDop) model [21]. We have demonstrated that this model can be used to estimate sea-state-induced Doppler shifts (hereafter referred to as wave Doppler) with relatively higher accuracy compared with the empirical models mentioned earlier. Based on the DPDop model, we have implemented wave Doppler correction and derived radial OSC velocities from Sentinel-1 SAR Doppler shifts. The SAR retrievals are in good agreement with HF radar measurements, with a bias of −0.04 m/s and a RMSE of 0.15 m/s [22]. In addition to wave Doppler, nongeophysical Doppler shifts are also very important for radial current retrieval and need to be accurately calculated [11], [23], [24].

Although SAR Doppler shift measurements have been used to retrieve radial OSC velocity during nonstorm events, no relevant investigations under hurricane conditions have been reported. In this study, for the first time, we aim to address this issue by retrieving radial OSC velocities from Sentinel-1 SAR Doppler shifts acquired over the outer core regions of Hurricane Maria. The results of the radial current retrieval are evaluated using HF radar measurements. Note that the radial velocity (RVL) is only one component of the OSC.

The rest of this article is organized as follows. The datasets are described in Section II. The details of radial current retrieval, results and validations are presented in Section III. Finally, Section IV concludes this article.

II. Datasets

To retrieve and evaluate radial OSC velocities under high wind conditions, we collected a Sentinel-1A (S-1A) SAR image acquired over Hurricane Maria in the Atlantic Ocean. Moreover, we also obtained HF radar-measured surface currents over the area of SAR imaging.

A. S-1A Level-1 and Level-2 Data

S-1A Level-1 data are a dual-polarization (VV, VH) SAR image acquired in interferometric wide (IW) swath mode. It is freely available at the Copernicus Open Access Hub.[1] The swath width is 250 km, and the spatial resolution in the range and azimuth directions for the IW mode are 5 and 20 m, respectively. The incidence angles over the three continuous subswaths are between 30° and 36° (near-swath), 36° and 42° (mid-swath), and 41° and 46° (far-swath). As shown in Fig. 1(a), the peripheral regions of Hurricane Maria were intercepted by S-1A on 26 September, 2017 at 22:57 UTC. In the SAR imaging area, there are three National Data Buoy Center (NDBC) buoys (#41025, #44014, and #44009) off the east coast of the USA. In this study, we extracted the RVL from the S-1A Level-2 ocean (OCN) product and converted RVL into the Doppler shift using the formula $f_{\rm dc} = -k_r U_{\rm rvl}/\pi$. Here, k_r is the electromagnetic wavenumber (for the C-band, $k_r = 112$ rad/m), and $U_{\rm rvl}$ is RVL. Fig. 1(b) illustrates S-1A SAR-measured Doppler shifts over Hurricane Maria.

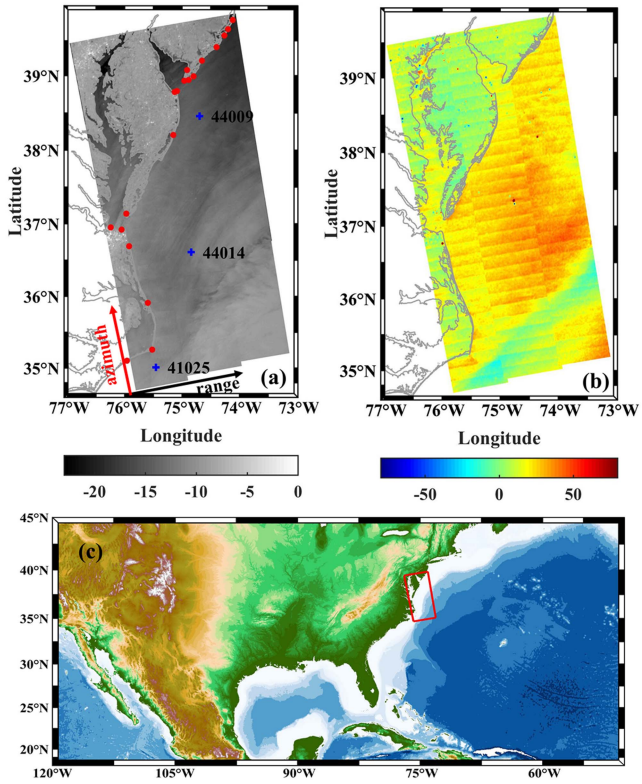

Fig. 1. (a) C-band S-1A VV-polarized SAR image acquired in IW swath mode over Hurricane Maria on 26 September, 2017 at 22:57 UTC. The colorbar denotes the normalized radar cross section at VV-polarization, in units of dB. Blue plus sign (+) represents the locations of the three NDBC buoys (#44009, #44014, and #41025). Red dots depict the geographic locations of the HF radar. Red and black arrows denote azimuth and range directions, respectively. (b) S-1A SAR-measured Doppler shifts from level-2 ocean (OCN) product. The colorbar represents the Doppler shift, in units of Hz. (c) Geographic location of the SAR image (red rectangle).

B. HF Radar Data

HF radars are shore-based microwave sensors that have been widely used to measure coastal surface current fields over a large region (∼300 km) in near real-time. HF radar transmits HF (3–50 MHz) electromagnetic waves that propagate along the ocean surface beyond the horizon and are backscattered by resonant waves known as "Bragg waves," which have a

[1][Online]. Available: https://scihub.copernicus.eu

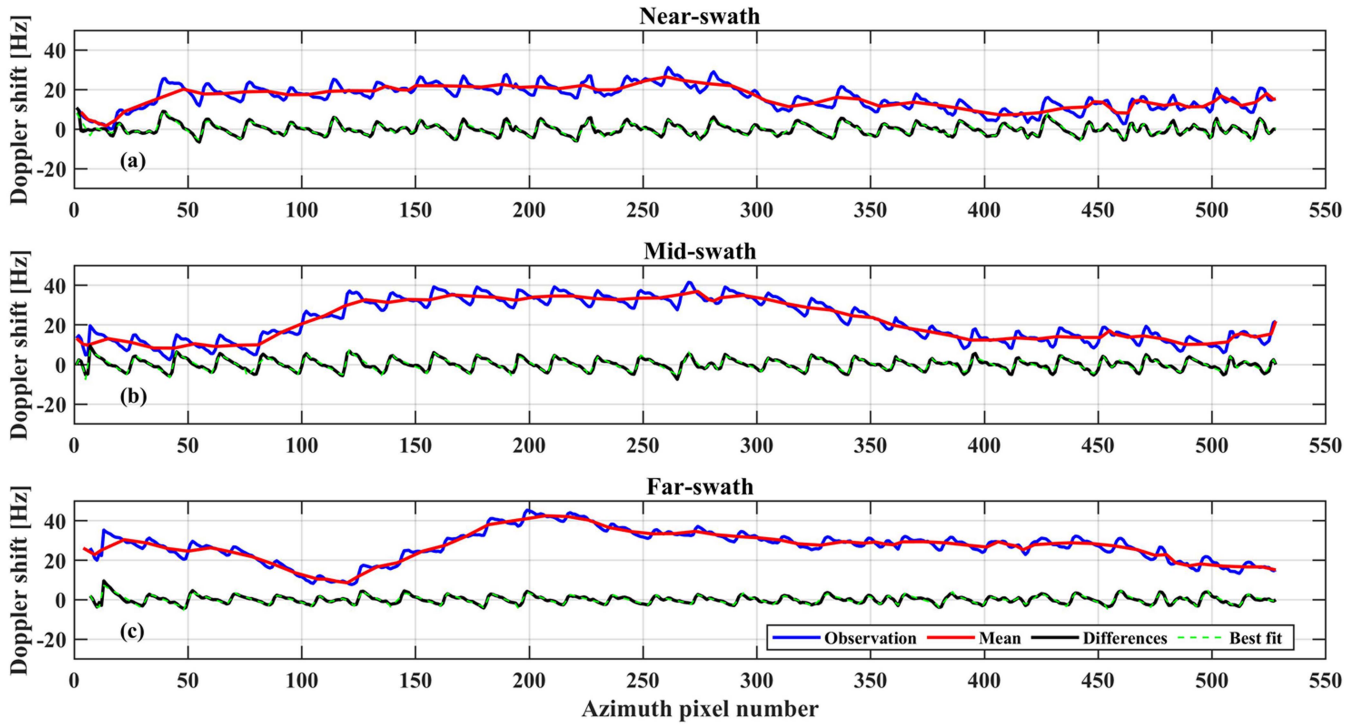

Fig. 2. Doppler shift profiles extracted from S-1A SAR IW scene acquired over Hurricane Maria on 26 September, 2017 at 22:57 UTC: Azimuth (along-track) Doppler shift profiles from observations (blue solid line), mean of the observations (red solid line), differences (observations—mean) (black solid line), and Doppler error due to the scalloping effect, estimated from a linear fit method (green dashed line), for (a) near-swath, (b) mid-swath, and (c) far-swath, respectively.

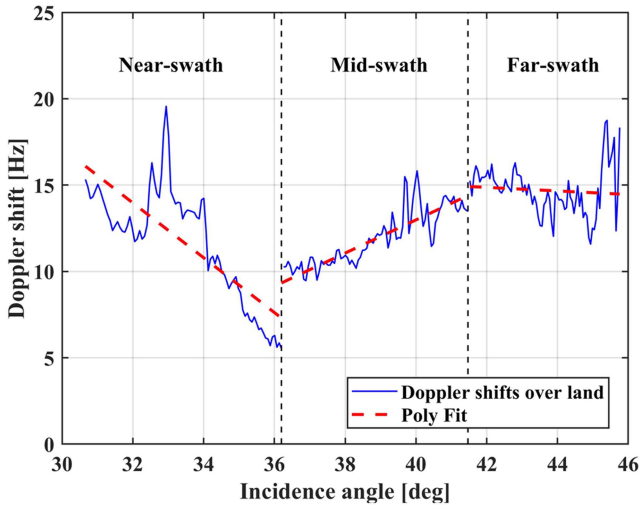

Fig. 3. Range (across-track) Doppler shift profile from observations (blue solid line) over the land within the SAR scene, and Doppler error (red dashed line) due to the antenna electronic mispointing and residual error estimated from the linear fit method for near-, mid-, and far-swaths, respectively.

wavelength half that of the radar wavelength. The displacement of the Bragg peaks in the Doppler spectrum from their expected positions is related to the surface current [25]. The accuracies of the HF radar current measurements typically range between 5 and 20 cm/s [26], [27], [28]. In this study, we use surface current measurements from the HF Radar Network (HFRNet)[2] to validate SAR-retrieval radial current velocities. The temporal and spatial resolutions of HF radar current products are 1 h and 6 km, respectively. The geographic locations of HF radar are shown in Fig. 1(a). As an essential component of Integrated Ocean Observing System, HF radars deployed on the East Coast of the United States provide OSC products with spatial resolutions of 1, 2, and 6 km. However, there is a tradeoff between spatial resolution and swath. A higher resolution (1 km) of OSC corresponds to a smaller observation area (45 km) of HF radar. There are only a few HF radar measurements available with a resolution of 1 or 2 km in the SAR acquisition. Therefore, in order to conduct a statistical validation, we compared the SAR-retrieved radial OSC with HF radar measurements at a resolution of 6 km.

[2][Online]. Available: https://hfrnet-tds.ucsd.edu/thredds/catalog.html

III. Results and Validation

A. Nongeophysical Doppler Shifts

SAR-measured instantaneous Doppler shifts (f_{dc}) are composed of various contributions, as expressed by

$$f_{dc} = f_{att} + f_{elec} + f_{sca} + f_{osc} + f_{ss} + \Delta f \quad (1)$$

where f_{att} is the Doppler shift caused by the satellite attitude variation, f_{elec} is the Doppler shift arising from antenna electronic mispointing, f_{sca} is the Doppler shift related to the scalloping effect in the azimuth direction. f_{osc} and f_{ss} are Doppler shifts induced by surface current and sea state, respectively. Δf is the total residual error and other unknown biases. Detailed descriptions of each component of (1) can be found in [12].

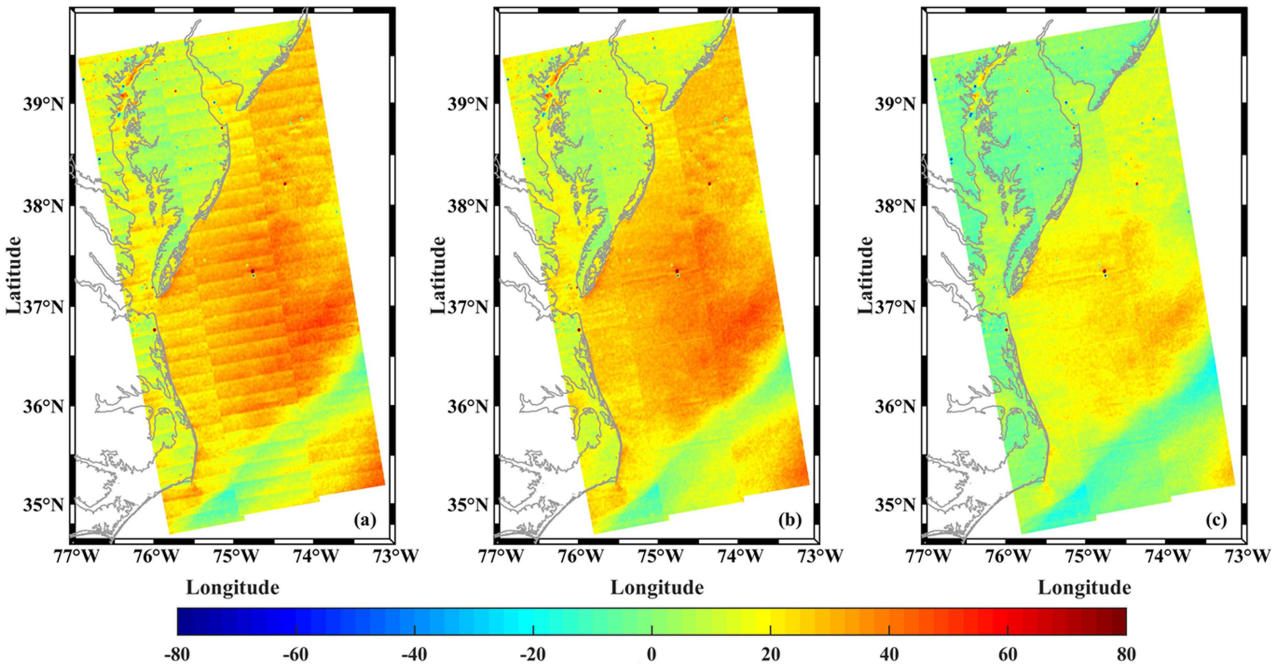

Fig. 4. (a) S-1A SAR-measured Doppler shifts over Hurricane Maria on 26 September, 2017 at 22:57 UTC, after removing the Doppler error due to the satellite attitude variations. (b) Doppler shifts after removing Doppler error due to the scalloping effect. (c) Doppler shifts after removing Doppler error caused by the antenna electronic mispointing and residual error. The colorbar represents the Doppler shift, in units of Hz.

In order to obtain a reliable estimate for the OSC velocity, the nongeophysical Doppler shifts ($f_{\text{att}}+f_{\text{elec}}+f_{\text{sca}}$) need to be accurately estimated and eliminated. Note that f_{att} has been involved in the S-1A Level-2 ocean (OCN) product. Fig. 2(a)–(c) shows azimuth Doppler shift profiles (blue solid lines) from observations for near-, mid-, and far-swaths, respectively. These observed Doppler shifts in the azimuth direction exhibit significant deviations from the "expected value" (0 Hz). These deviations are caused by the scalloping error associated with the antenna sweep motion in the S-1A TOPSAR acquisition mode. We first estimate the mean values (red solid lines) using adjacent Doppler shifts at peak and trough locations. Then, the differences (black solid lines) between observations and averages are calculated. Finally, we use a linear fitting method to estimate the Doppler shifts arising from the scalloping effect (f_{sca}, green dashed lines) for each pixel in the azimuth direction. Fig. 3 illustrates the range Doppler shift profiles (blue solid line) obtained from observations over the land for the three swaths. As shown in Fig. 3, distinct Doppler shift undulations (5.5–19.5 Hz) exist in each subswath and notable "jumps" are found between subswaths. The nonzero Doppler shifts over the land are related to antenna electronic mispointing and residual error. In this study, we use fitted Doppler shifts (red dashed line) over the land area within the SAR scene to estimate f_{elec} and Δf.

Fig. 4(a) shows the SAR-measured Doppler shifts after removing the contribution caused by the satellite attitude variation. Distinct scalloping patterns in the azimuth direction are clearly present. After subtracting the Doppler error due to the scalloping effect, no prominent stripes are visible, as shown in Fig. 4(b). Yet, there are still abnormal Doppler shifts with large values present in both the land area and the offshore region. These shifts are associated with changes in the antenna beam pattern and the residual error. Fig. 4(c) presents the Doppler shifts after removing contributions from antenna electronic mispointing and the residual error.

B. Wave Doppler

Under hurricane conditions, strong winds generate wind waves and associated swells with significant orbital motions. High sea states can significantly contribute to the Doppler shift, in addition to the underlying surface currents. Therefore, we need to accurately estimate wave Doppler (f_{ss}) and eliminate this component from the SAR measurements.

Fig. 5(a) shows the retrieved wind speeds using the S-1A dual-polarization SAR image of Hurricane Maria, based on the algorithm proposed in [29]. The spatial resolution of the retrieved wind speeds is 1 km. S-1A Level-2 OCN product provides wind directions from both SAR retrieval and ECMWF reanalysis. In this study, we use wind directions from ECMWF instead of SAR because the former is more accurate. Although the S-1A SAR image only captured a peripheral area of Hurricane Maria's structure, high winds (>20 m/s) are observed to the east of Hatteras Island (Latitude: 35°24'17.99" N, Longitude: −75°29'7.79" W), with a maximum wind speed of 28.7 m/s. Fig. 5(b) presents the significant wave heights of Hurricane Maria derived from WAVEWATCH III (WW3) on 26 September, 2017 at 23:00 UTC. The spatial resolution of the WW3 simulation for the significant wave height is 1/15°. As shown in Fig. 5(b), large significant wave heights (6–8 m) are clearly shown in the high wind region. The blank area in Fig. 5(b) represents the missing significant wave heights

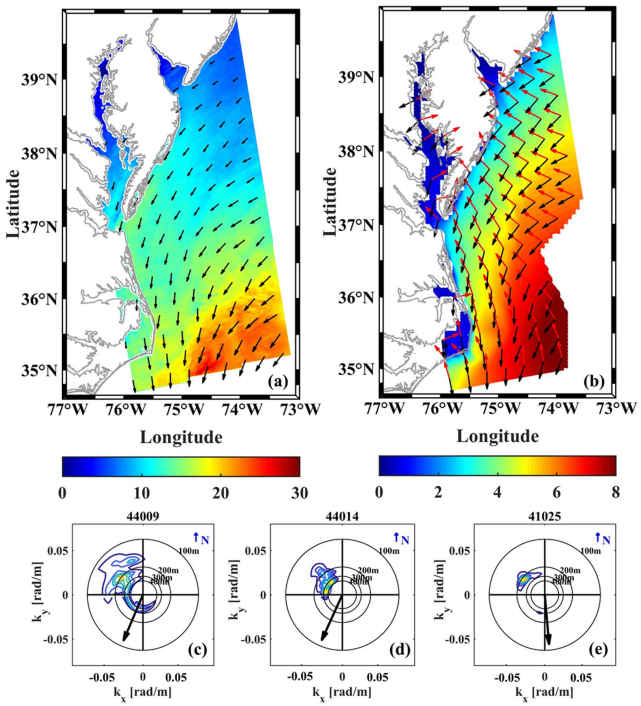

Fig. 5. (a) Ocean surface wind field retrieved from S-1A dual-polarization (VV, VH) SAR image acquired in IW swath mode over Hurricane Maria on 26 September, 2017 at 22:57 UTC. Black arrows represent ECMWF wind directions. The colorbar represents the wind speed, in units of m/s. (b) Significant wave height of Hurricane Maria derived from WAVEWATCH III (WW3) on 26 September, 2017 at 23:00 UTC. Black and red arrows denote the ECMWF wind directions and WW3 wave directions, respectively. The colorbar represents the significant wave height, in units of m. (c)–(e) Are directional wave spectra measured by NDBC buoys [#44009, #44014, and #41025 as shown in Fig. 1(a)] on 26 September, 2017 at 23:00 UTC. Black arrows in (c)–(e) represent the average wind direction measured by the buoy over an 8-min period. k_x and k_y stand for azimuth and range wavenumbers, respectively.

of WW3. Moreover, we also observe significant differences between wind directions (black arrows) and wave directions (red arrows), indicating the prevalence of swell or mixed sea states. This is confirmed by the directional wave spectra measured by three NDBC buoys, as shown in the Fig. 5(c)–(e). Tri-, bi-, and mono-modal spectra are explicitly exhibited for buoys #44009, #44014, and #41025, respectively. Black arrows in Fig. 5(c)–(e) represent wind directions, which show notable deviations from the peak wave directions, particularly for buoys #44014 and #41025. As shown in the Fig. 5(c)–(e), the wind directions measured by three NDBC buoys (#44009, #44014, and #41025) are 22°, 24°, and 355°, respectively. The wind directions from SAR are 48°, 37°, and 354°, and from ECMWF are 45°, 20°, and 349°, respectively. Compared with buoy measurements, the RMSEs of wind direction are 7.7° and 9.4° for ECMWF and SAR, respectively. Recent studies have shown that wind directions can be directly estimated from dual-polarization (VV + VH) SAR images acquired during hurricanes, using either the Hann window function [30] or the local gradient method [31]. The RMSEs of wind direction derived from these two methods are 20.24° and 13.30°, respectively. In general, ECMWF reanalysis data or a high-resolution limited area model provide background information for SAR wind speed retrieval. It should be noted that SAR has the potential to derive the background field. For example, we can use cross- and dual-polarization SAR images to generate initial estimates of the u and v wind components.

We calculate wave Doppler based on our recent model, the DPDop model [22]. The DPDop model can estimate each component of Doppler velocity, including the velocities of resonant Bragg waves and breakers, as well as the contributions of tilt and hydrodynamic modulations due to long surface waves to the Doppler velocity. The DPDop model development was not based on the assumption of a fully developed wind-wave, a pure swell, or hybrid wave systems. Therefore, it has the capability of yielding wave Doppler caused by a mixed sea state, given the surface wind field, characteristic wave parameters (e.g., significant wave height, mean wave direction, and mean wavenumber), or 2-D wave spectra, and radar configurations. The upper limit on the wind speed in the DPDop model is 30 m/s. Thus, this model can be used to estimate the contributions of orbital motions of the waves to the Doppler shift, at least for the case of Hurricane Maria. The inputs of the DPDop model are ocean surface wind fields, characteristic wave parameters (significant wave height, mean wave direction, and mean wavenumber) from WW3, and radar parameters (incidence angle and radar look direction). DPDop model outputs Doppler shifts induced by wind waves and swell, as shown in Fig. 6(a). Fig. 6(b) presents the Doppler shifts after removing the sea state effect using the DPDop model. Note that the Doppler shifts shown in Fig. 6(b) are only related to OSC because the effects of nongeophysical terms and sea state have been removed.

C. Radial Current Retrievals and Validations

As the current-induced Doppler shift (f_{osc}) is derived, we estimate the radial OSC velocity (U_{rvl}) via the following formula:

$$U_{\text{rvl}} = -\frac{\pi f_{\text{osc}}}{k_r \sin\theta} \tag{2}$$

where k_r is the electromagnetic wavenumber, and θ is the radar incidence angle. Note that U_{rvl} is positive or negative when the scattering facets on the ocean surface move away from or toward the radar, respectively. The retrieved radial OSC velocities on 26 September, 2017 at 22:57 UTC, with a resolution of 1 km, are shown in Fig. 6(c). The strong radial currents appear in high-wind areas with a maximum of 0.66 m/s. To evaluate the radial surface currents retrieved by SAR, we collected the HF radar current measurements (with a resolution of 6 km) on 26 September, 2017 at 23:00 UTC. These measurements were then projected into the radial direction, as shown in Fig. 6(d). Prior to evaluation, we resample the spatial resolution of SAR-derived currents to 6 km to ensure consistency with that of HF radar-measured currents. Fig. 7 presents comparisons of SAR-retrieved radial OSC velocities and HF radar measurements, both without and with the removal of wave Doppler. As shown in Fig. 7(a), significant errors in the retrieved OSC velocity occur when the effects of sea state on Doppler shift are not eliminated. In contrast, as displayed in Fig. 7(b), the bias and RMSE decrease significantly after eliminating the influence of sea state using the

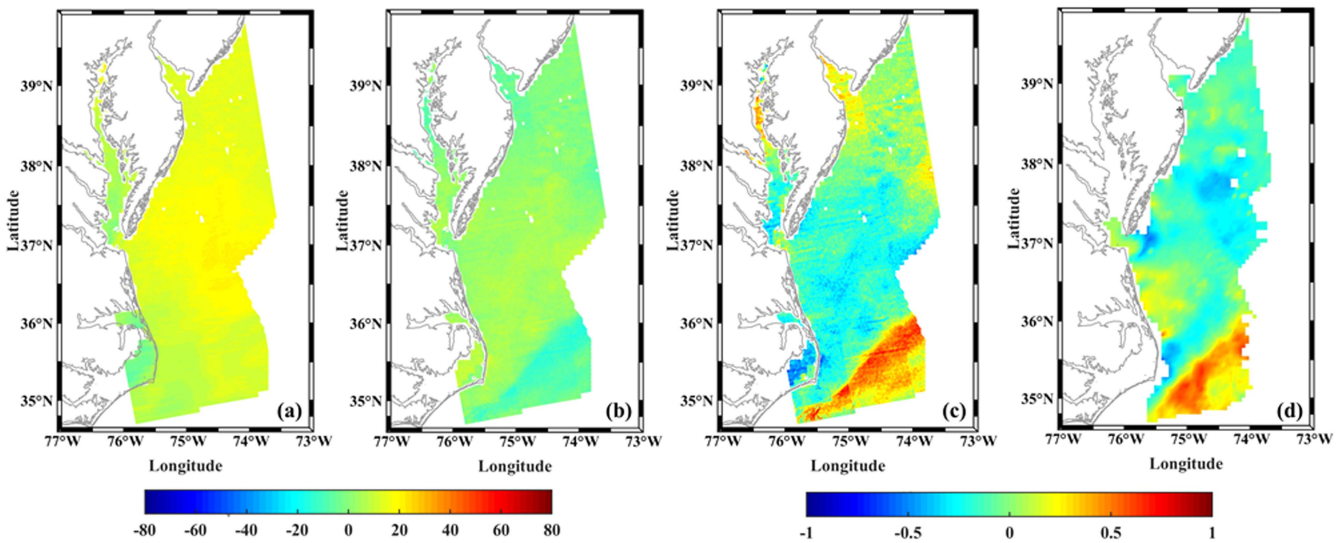

Fig. 6. (a) Estimated wave Doppler using DPDop model, (b) S-1A SAR Doppler shifts over Hurricane Maria on 26 September, 2017 at 22:57 UTC, after removing sea state effect (wave Doppler correction) using the DPDop model. The colorbar in Fig. 6(a) and (b) represent the Doppler shift, in units of Hz. (c) Retrieved radial surface current velocities from Doppler shifts as shown in Fig. 6(b), and (d) HF radar-measured radial surface current velocities on 26 September, 2017 at 23:00 UTC. The colorbar in Fig. 6(c) and (d) represent the radial surface current velocities, in units of m/s.

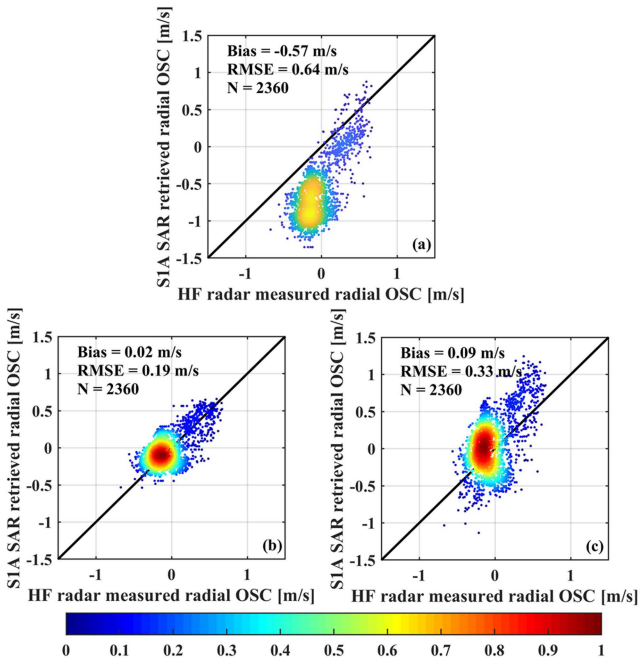

Fig. 7. Comparisons of SAR-retrieved radial OSC velocities and collocated HF radar measurements: (a) Without removal of wave Doppler, (b) with removal of wave Doppler using DPDop model, and (c) with removal of wave Doppler using CDOP model. The color bar represents the density of the point distribution.

DPDop model. The bias is 0.02 m/s, and the RMSE is 0.19 m/s. When the radial OSC velocities are larger than 0.2 m/s, the bias and RMSE are −0.07 m/s and 0.21 m/s, respectively. Compared with Fig. 7(b), the bias and RMSE of the retrieved radial OSC velocities in Fig. 7(c) are much larger, with values of 0.09 and 0.33 m/s, respectively. This is because the CDOP model ignores the contribution of swell to the Doppler shift [32]. Therefore, the Doppler shift induced by sea state needs to be precisely estimated and corrected in order to obtain reliable radial OSC velocity, especially under high wind conditions. The differences between SAR retrievals and HF radar measurements are likely related to inaccurate Doppler shift corrections for nongeophysical and geophysical terms, as well as uncertainty estimates for HF radar current observations.

IV. Discussion and Conclusion

This is the first attempt to retrieve radial OSC velocities in the outer core regions of Hurricane Maria using the Doppler shifts in a S-1A SAR image. Prior to retrieving radial surface currents, we estimate the Doppler shifts caused by the scalloping effect, the antenna electronic mispointing and residual error, and sea state. These estimates, along with those related to satellite attitude variation, are eliminated from the observed Doppler shifts. We compare SAR-retrieved radial OSC velocities with HF radar measurements. The bias and RMSE are 0.02 and 0.19 m/s, respectively.

The errors in radial OSC retrieval are largely attributed to potentially inaccurate estimates of nongeophysical and geophysical Doppler shifts. For example, the imprecise satellite attitude and orbit parameters can potentially lead to unreliable estimates of geometric Doppler shift (f_{att}). Moreover, an inaccurate antenna model may also result in an incorrect Doppler shift (f_{elec}) associated with antenna electronic mispointing. Although the biases caused by inaccurate geometry and electronic mispointing can be corrected using the nonzero Doppler shift measurements over the land area within SAR images, residual error may still exist. In this study, we apply the DPDop model to estimate wave Doppler using the surface wind field, characteristic wave parameters, and radar configurations. The potential errors in SAR-retrieved wind speeds, ECMWF wind directions,

and WW3 model-simulated significant wave heights are likely to affect the accurate prediction of geophysical Doppler shift caused by wind waves and swells. Moreover, uncertainties in the HF radar current measurements may also lead to discrepancies in current comparisons. Radial surface current velocities derived from SAR and HF radar observations include the contribution of the wave-induced Stokes drift. Yet, the magnitude of Stokes drift is discrepant due to different current measurement depths for SAR ($<$0.01 m) and HF radar (1–2 m). The difference between SAR current retrievals and HF radar measurements is partly related to the Stokes drift.

Under extreme weather conditions, high sea states (wind waves and swells) can cause significant contributions to Doppler shifts. Therefore, Doppler shifts arising from the sea state need to be accurately estimated and eliminated. In this study, we use the DPDop model to correct the wave Doppler in the outer core regions of Hurricane Maria. In these areas, the maximum wind speed is 28.7 m/s. Note that the upper limit for wind speed in the DPDop model is 30 m/s. This suggests that the DPDop model is applicable to correct wave Doppler for weak storms ($\leq$30 m/s). In the future, we plan to expand the wind speed range of this model and calculate wave Doppler in the eyewall region of strong hurricanes. As such, strong radial surface currents ($\sim$2 m/s) may be derived from SAR Doppler shift measurements. Note that the S-1A SAR intercepted Hurricane Maria in the coastal region. Thus, we can use land cover data in this SAR image to correct the bias linked to nongeophysical Doppler shifts ($f_{\text{att}} + f_{\text{elec}}$) and residual error ($\Delta f$). For SAR scenes acquired in land-free open ocean areas, obtaining reliable radial OSC velocities from SAR-measured Doppler shift is challenging. A recent study has presented an approach to estimate f_{elec} in land-free SAR images by analyzing seasonal Doppler shift variations using multitemporal SAR images acquired in the same region [33]. The feasibility of this method needs further evaluation. We will also continue to explore radial OSC measurements using SAR observations acquired under storm conditions and in open ocean areas.

REFERENCES

[1] L. K. Shay, R. L. Elsberry, and P. G. Black, "Vertical structure of the ocean current response to a hurricane," *J. Phys. Oceanogr.*, vol. 19, pp. 649–669, 1989.

[2] T. B. Sanford, J. F. Price, and J. B. Girton, "Upper-ocean response to hurricane Frances (2004) observed by profiling EM-APEX floats," *J. Phys. Oceanogr.*, vol. 41, pp. 1041–1056, 2011, doi: 10.1175/2010JPO4313.1.

[3] S. M. Glenn, "Stratified coastal ocean interactions with tropical cyclones," *Nature Commun.*, vol. 7, 2016, Art. no. 10887, doi: 10.1038/ncomms10887.

[4] S. Mitarai and J. C. McWilliams, "Wave glider observations of surface winds and currents in the core of typhoon Danas," *Geophys. Res. Lett.*, vol. 43, pp. 11,312–11,319, 2016, doi: 10.1002/2016GL071115.

[5] G. R. Foltz, C. Zhang, C. Meinig, J. A. Zhang, and D. Zhang, "An unprecedented view inside a hurricane," *Eos*, vol. 103, 2022, doi: 10.1029/2022EO220228.

[6] T. Miles, "Uncrewed ocean gliders and saildrones support hurricane forecasting and research," *Oceanography*, vol. 34, pp. 78–81, 2021, doi: 10.5670/oceanog.2021.supplement.02-28.

[7] Y.-C. Chang, R.-S. Tseng, P. C. Chu, J.-M. Chen, and L. R. Centurioni, "Observed strong currents under global tropical cyclones," *J. Mar. Syst.*, vol. 156, pp. 33–40, 2016, doi: 10.1016/j.jmarsys.2016.03.001.

[8] S. Fan et al., "Observed ocean surface winds and mixed layer currents under tropical cyclones: Asymmetric characteristics," *J. Geophys. Res.: Oceans*, vol. 127, 2022, Art. no. e2021JC017991, doi: 10.1029/2021JC017991.

[9] B. Chapron, F. Collard, and F. Ardhuin, "Direct measurements of ocean surface velocity from space: Interpretation and validation," *J. Geophys. Res.*, vol. 110, 2005, Art. no. C07008, doi: 10.1029/2004JC002809.

[10] J. A. Johannessen et al., "Direct ocean surface velocity measurements from space: Improved quantitative interpretation of Envisat ASAR observations," *Geophys. Res. Lett.*, vol. 35, 2008, Art. no. L22608, doi: 10.1029/2008GL035709.

[11] M. W. Hansen, F. Collard, K.-F. Dagestad, J. A. Johannessen, P. Fabry, and B. Chapron, "Retrieval of sea surface range velocities from Envisat ASAR Doppler centroid measurements," *IEEE Trans. Geosci. Remote Sens.*, vol. 49, no. 10, pp. 3582–3592, Oct. 2011, doi: 10.1109/TGRS.2011.2153864.

[12] A. Moiseev, J. A. Johannessen, and H. Johnsen, "Toward retrieving reliable ocean surface currents in the coastal zone from the Sentinel-1 Doppler shift observations," *J. Geophys. Res.: Oceans*, vol. 127, 2022, Art. no. e2021JC018201, doi: 10.1029/2021JC018201.

[13] A. Moiseev, H. Johnsen, M. W. Hansen, and J. A. Johannessen, "Evaluation of radial ocean surface currents derived from Sentinel-1 IW Doppler shift using coastal radar and Lagrangian surface drifter observations," *J. Geophys. Res.: Oceans*, vol. 125, 2020, Art. no. e2019JC015743, doi: 10.1029/2019JC015743.

[14] P. J. Bowyer and A. W. Macafee, "The theory of trapped-fetch waves with tropical cyclones–An operational perspective," *Weather Forecasting*, vol. 20, pp. 229–244, 2005.

[15] I. R. Young and J. Vinoth, "An 'extended fetch' model for the spatial distribution of tropical cyclone wind-waves as observed by altimeter," *Ocean Eng.*, vol. 70, pp. 14–24, 2013.

[16] L. H. Holthuijsen, M. D. Powell, and J. D. Pietrzak, "Wind and waves in extreme hurricanes," *J. Geophys. Res.: Oceans*, vol. 117, 2012, Art. no. C09003, doi: 10.1029/2012JC007983.

[17] K. Hu and Q. Chen, "Directional spectra of hurricane-generated waves in the Gulf of Mexico," *Geophys. Res. Lett.*, vol. 38, 2011, Art. no. L19608, doi: 10.1029/2011GL049145.

[18] Y.-C. Chang, G.-Y. Chen, R.-S. Tsen, L. R. Centurioni, and P. C. Chu, "Observed near-surface flows under all tropical cyclone intensity level using drifter in the northwestern pacific," *J. Geophys. Res: Oceans.*, vol. 118, pp. 2367–2377, 2013, doi: 10.1002/jgrc/20187.

[19] K.-M. Kang, D.-J. Kim, S. H. Kim, and W. M. Moon, "Doppler velocity characteristics during tropical cyclones observed using ScanSAR raw data," *IEEE Trans. Geosci. Remote Sens.*, vol. 54, no. 4, pp. 2343–2355, Apr. 2016, doi: 10.1109/TGRS.2015.2499443.

[20] A. Moiseev, H. Johnsen, J. A. Johannessen, F. Collard, and G. Guitton, "On removal of sea state contribution to Sentinel-1 Doppler shift for retrieving reliable ocean surface current," *J. Geophys. Res: Oceans.*, vol. 125, 2020, Art. no. e2020JC016288, doi: 10.1029/2020JC016288.

[21] V. Kudryavtsev, S. Fan, B. Zhang, B. Chapron, J. A. Johannessen, and A. Moiseev, "On the use of dual co-polarized radar data to derive a sea surface Doppler model –Part 1: Approach," *IEEE Trans. Geosci. Remote Sens.*, vol. 61, 2023, Art. no. 4201013, doi: 10.1109/TGRS.2023.3235829.

[22] S. Fan, B. Zhang, A. Moiseev, V. Kudryavtsev, J. A. Johannessen, and B. Chapron, "On the use of dual co-polarized radar data to derive a sea surface Doppler model–part 2: Simulation and validation," *IEEE Trans. Geosci. Remote Sens.*, vol. 61, 2023, Art. no. 4202009, doi: 10.1109/TGRS.2023.3246771.

[23] A. Elyouncha, L. E. B. Eriksson, and H. Johnsen, "Direct comparison of sea surface velocity estimated from Sentinel-1 and TanDEM-X SAR data," *IEEE J. Sel. Topics Appl. Earth Observ. Remote Sens.*, vol. 15, pp. 2425–2436, 2022, doi: 10.1109/JSTARS.2022.3158190.

[24] A. Martin, C. P. Gommenginger, B. Jacob, and J. Staneva, "First multi-year assessment of sentinel-1 radial velocity products using HF radar currents in a coastal environment," *Remote Sens. Environ.*, vol. 268, 2022, Art. no. 112758, doi: 10.1016/j.rse.2021.112758.

[25] R. H. Stewart and J. W. Joy, "HF radio measurements of surface current," *Deep Sea Res.*, vol. 21, pp. 1039–1049, 1974, doi: 10.1016/0011-7471(74)90066-7.

[26] P. Lorente, J. Soto-Navarro, E. A. Fanjul, and S. Piedracoba, "Accuracy assessment of high frequency radar current measurements in the Strait of Gibraltar," *J. Oper. Oceanogr.*, vol. 7, no. 2, pp. 59–73, 2014, doi: 10.1080/1755876X.2014.11020300.

[27] A. Kalampokis, M. Uttieri, P.-M. Poulain, and E. Zambianchi, "Validation of HF radar-derived currents in the Gulf of Naples with Lagrangian data," *IEEE Geosci. Remote Sens. Lett.*, vol. 13, no. 10, pp. 1452–1456, Oct. 2016, doi: 10.1109/LGRS.2016.2591258.
[28] B. Emery and L. Washburn, "Uncertainty estimates for SeaSonde HF radar ocean current observations," *J. Atmospheric Ocean. Technol.*, vol. 36, no. 2, pp. 231–247, 2019, doi: 10.1175/JTECH-D-18-0104.1.
[29] A. A. Mouche, B. Chapron, B. Zhang, and R. Husson, "Combined co- and cross-polarized SAR measurements under extreme wind conditions," *IEEE Trans. Geosci. Remote Sens.*, vol. 55, no. 12, pp. 6746–6755, Dec. 2017, doi: 10.1109/TGRS.2017.2732508.
[30] W. Ni, A. Stoffelen, and K. Ren, "Tropical cyclone wind direction retrieval from dual-polarized SAR imagery using histogram of oriented gradients and Han window function," *IEEE J. Sel. Topics Appl. Earth Observ. Remote Sens.*, vol. 16, pp. 878–888, 2023, doi: 10.1109/JSTARS.2022.3230441.
[31] S. Fan, B. Zhang, A. A. Mouche, W. Perrie, J. A. Zhang, and G. Zhang, "Estimation of wind direction in tropical cyclones using C-band dual-polarization synthetic aperture radar," *IEEE Trans. Geosci. Remote Sens.*, vol. 58, no. 2, pp. 1450–1462, Feb. 2020, doi: 10.1109/TGRS.2019.2946885.
[32] A. A. Mouche et al., "On the use of Doppler shift for sea surface wind retrieval from SAR," *IEEE Trans. Geosci. Remote Sens.*, vol. 50, no. 7, pp. 2901–2909, Jul. 2012, doi: 10.1109/TGRS.2011.2174998.
[33] Z. Yang et al., "Extrapolation of electromagnetic pointing error corrections for Sentinel-1 Doppler currents from land areas to the open ocean," *Remote Sens. Environ.*, vol. 297, 2023, Art. no. 113788, doi: 10.1016/j.rse.2023.113788.

Shengren Fan received the B.S. degree in atmosphere sciences, M.S. and Ph.D. degrees in marine meteorology from the Nanjing University of Information Science and Technology, Nanjing, China, in 2016, 2019, and 2022, respectively.

He is currently a Researcher with the Satellite Oceanography Laboratory, Russian State Hydro Meteorological University, St. Petersburg, Russia. His research interests include microwave scattering numerical simulation, tropical cyclone remote sensing through dual-polarization synthetic aperture radar and ocean current retrieved from SAR measurements.

Biao Zhang (Senior Member, IEEE) received the B.S. degree in surveying and mapping engineering from the China University of Petroleum, Dongying, China, in 2003, and the Ph.D. degree in physical oceanography from the Institute of Oceanology, Chinese Academy of Sciences, Qingdao, China, in 2008.

He was with the Bedford Institute of Oceanography, Dartmouth, NS, Canada, from 2008 to 2011, where he was a Postdoctoral Fellow and involved in developing synthetic aperture radar ocean surface wave and wind retrieval algorithms and products. He is currently a Professor with the School of Marine Sciences, Nanjing University of Information Science and Technology, Nanjing, China. His research interests include satellite remote sensing of marine dynamic environment and tropical cyclone, air–sea interaction under extreme weather conditions, Arctic sea ice monitoring by active and passive microwave sensors, and radar constellation mission.

Dr. Zhang was a recipient of the Visiting Fellow Scholarship of Natural Sciences and Engineering Research Council of Canada, the first award of Science and Technology from Jiangsu Province in 2017, the first award of Ocean Science and Technology from the State Oceanic Administration of China, the second award of Natural Science from the Ministry of Education of China in 2014, and the Outstanding Young Scientist Award by National Science Foundation of China in 2016. He was selected as "six talent peaks" of Jiangsu Province in 2018.

Vladimir Kudryavtsev received the Ph.D. and Senior Doctorate degrees in geophysics/marine physics from the Marine Hydrophysical Institute (MHI), Sevastopol, Russia, in 1981 and 1991, respectively.

In 1976, he joined MHI. From 2005 to 2013, he was with the Nansen Center, St. Petersburg, Russia. Since 2002, he has been a Professor with Russian State Hydro Meteorological University, St. Petersburg, where he is currently the Head of the Satellite Oceanography Laboratory. He is also a part-time Principal Scientist with MHI, and until June 2016 also held a part-time Senior Position II with the Nansen Center, Bergen, Norway. His current research interests include air–sea interaction, atmospheric and oceanic boundary layers, and radar and optical imaging of the ocean surface.

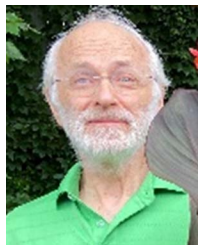

William Perrie received the B.S. degree in physics from the University of Toronto, Toronto, ON, Canada, in 1973, and the Ph.D. degree in meteorology and oceanography from the Massachusetts Institute of Technology, Cambridge, MA, USA, in 1979.

He was a Postdoctoral Fellow in oceanography and mathematics with the University of British Columbia, Vancouver, BC, Canada, and the National Center for Atmospheric Research, Boulder, CO, USA. He is currently a Senior Scientist with the Bedford Institute of Oceanography, Dartmouth, NS, Canada, and an Adjunct Professor with Dalhousie University, Halifax, NS. His research interests include the modeling of ocean waves, air–sea fluxes, coupled atmosphere ocean interactions and impacts of climate change on these variables, and field measurements via remote sensing and in situ of winds, waves, and currents.